

**Electronic supplementary Information:**

**Enhanced Photophysical properties of plasmonic-magnetic metal-alloyed semiconductor heterostructure nanocrystals :  
A case study for Ag@Ni/Zn<sub>1-x</sub>Mg<sub>x</sub>O system**

Sumana Paul, Sirshendu Ghosh\*, Manas Saha and S. K. De\*

**Table S1: Calculated Crystallite size, micro strain calculated from Williamson Hall (W-H) plot of different Mg alloyed ZnO nanocrystals:**

Sample	Crystallite sizes (D) calculated from W-H plot (nm)	Microstrain ( $\eta$ ) calculated from W-H plot
ZnO	19.85±1.86	-0.00262±0.00202
Zn <sub>0.95</sub> Mg <sub>0.05</sub> O	21.30±3.32	-0.00338±0.00121
Zn <sub>0.9</sub> Mg <sub>0.1</sub> O	18.33±2.16	-0.00362±0.0017
Zn <sub>0.8</sub> Mg <sub>0.2</sub> O	10.04±1.62	-0.01086±0.00446
Zn <sub>0.7</sub> Mg <sub>0.3</sub> O	11.62±3.53	-0.00871±0.00783
Zn <sub>0.6</sub> Mg <sub>0.4</sub> O	13.61±2.15	-0.00549±0.0032
Zn <sub>0.5</sub> Mg <sub>0.5</sub> O	1.21±0.58	-0.19289±0.13522

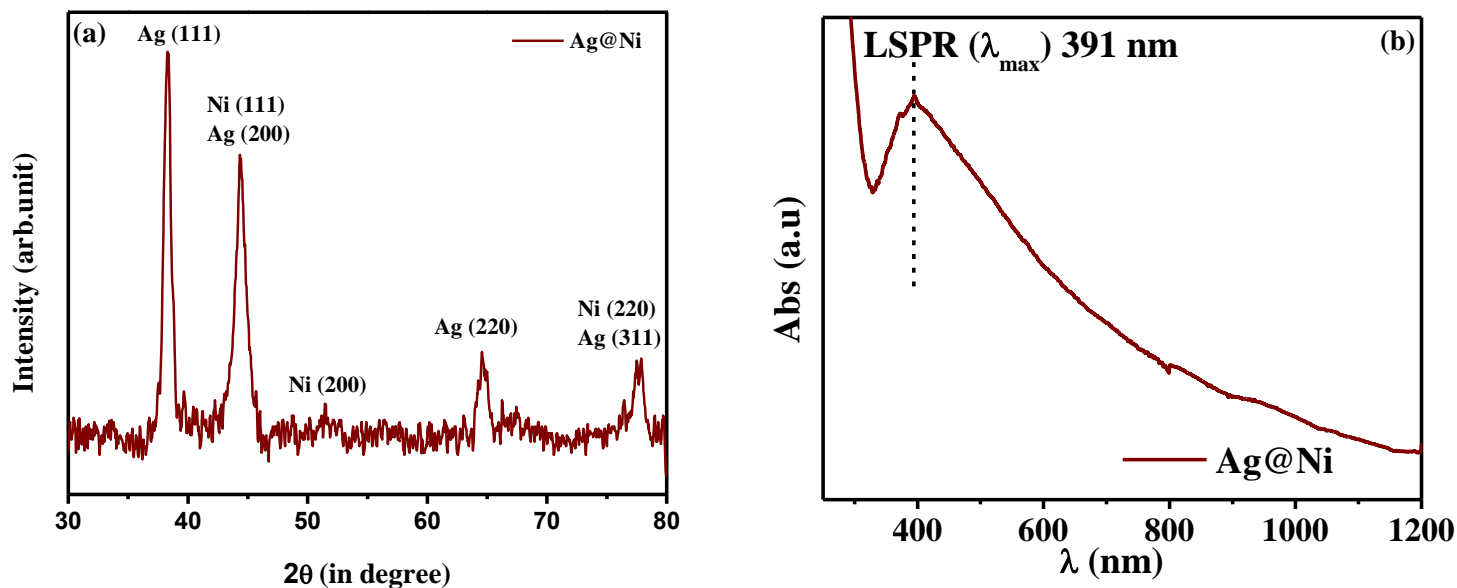


**Fig. S1:** (a) XRD pattern of as-synthesized Ag@Ni core shell structure. (b) Absorbance spectra of the core-shell in TCE solvent shows the plasmon peak of Ag has broadened and blue shifted.

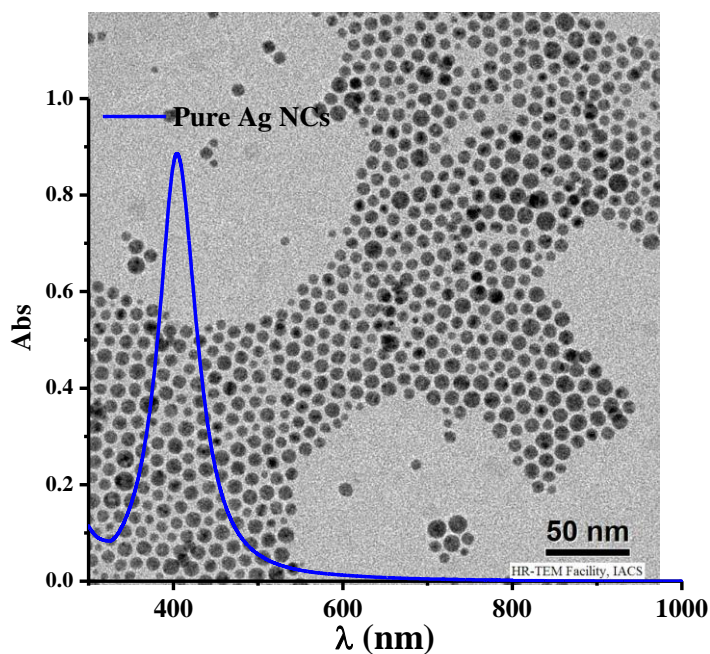


**Fig. S1 (c):** TEM image of monodisperse Ag NCs used as seeds ( $9.6 \pm 1.7$  nm). LSPR absorbance was found at 410 nm.

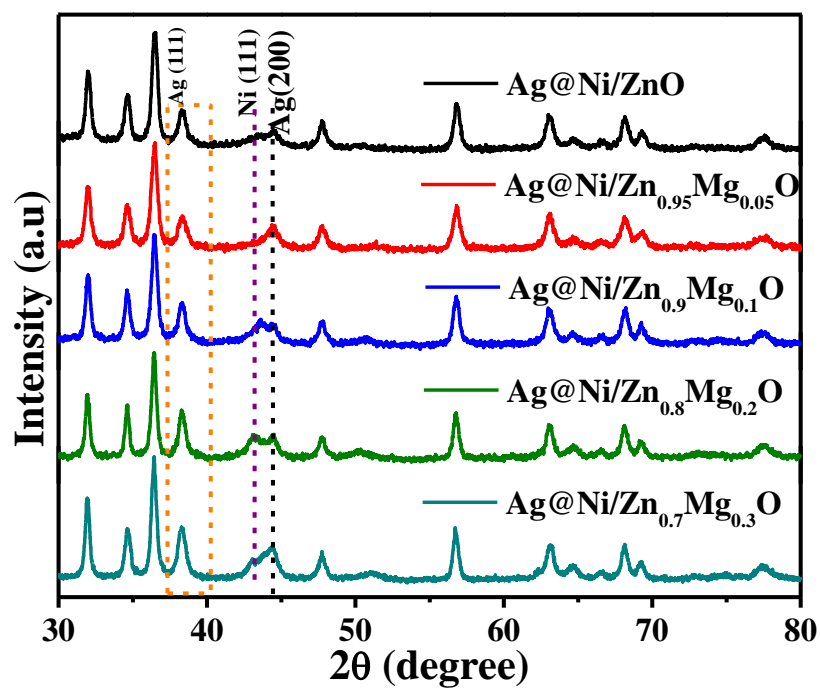


Fig. S2: XRD pattern of Ag@Ni/Zn<sub>1-x</sub>Mg<sub>x</sub>O heterostructures.

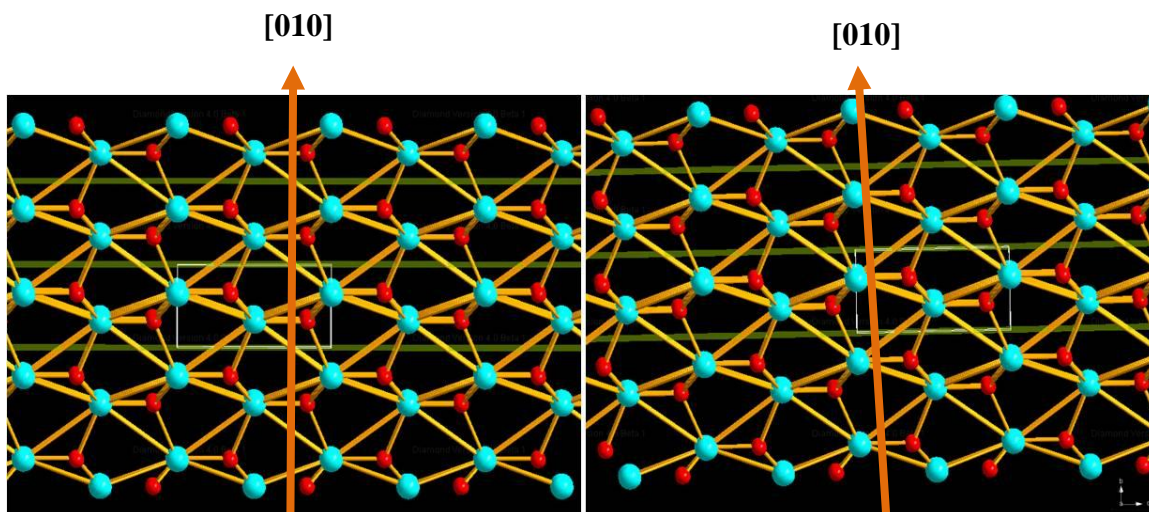
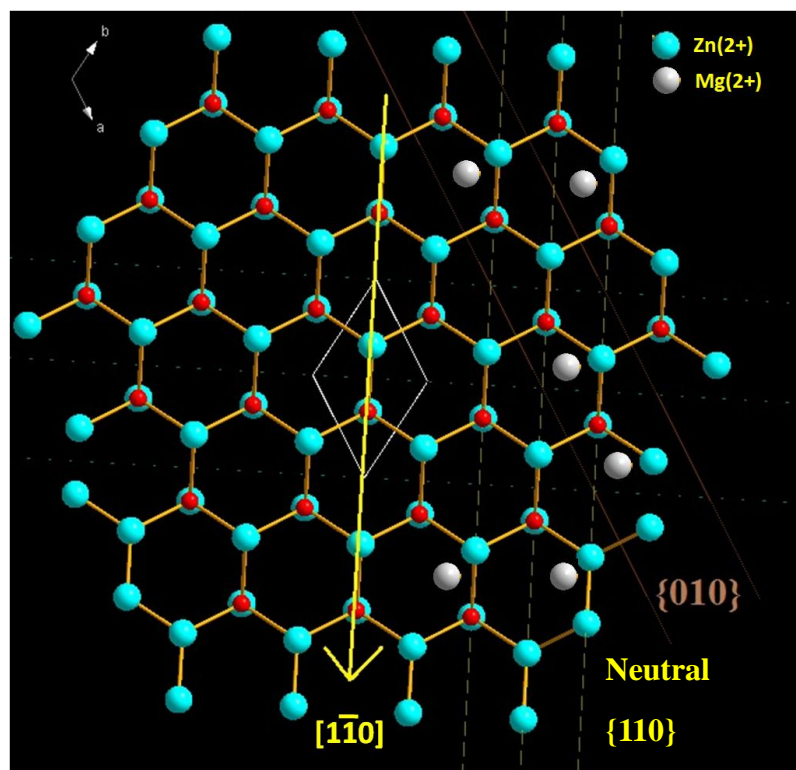
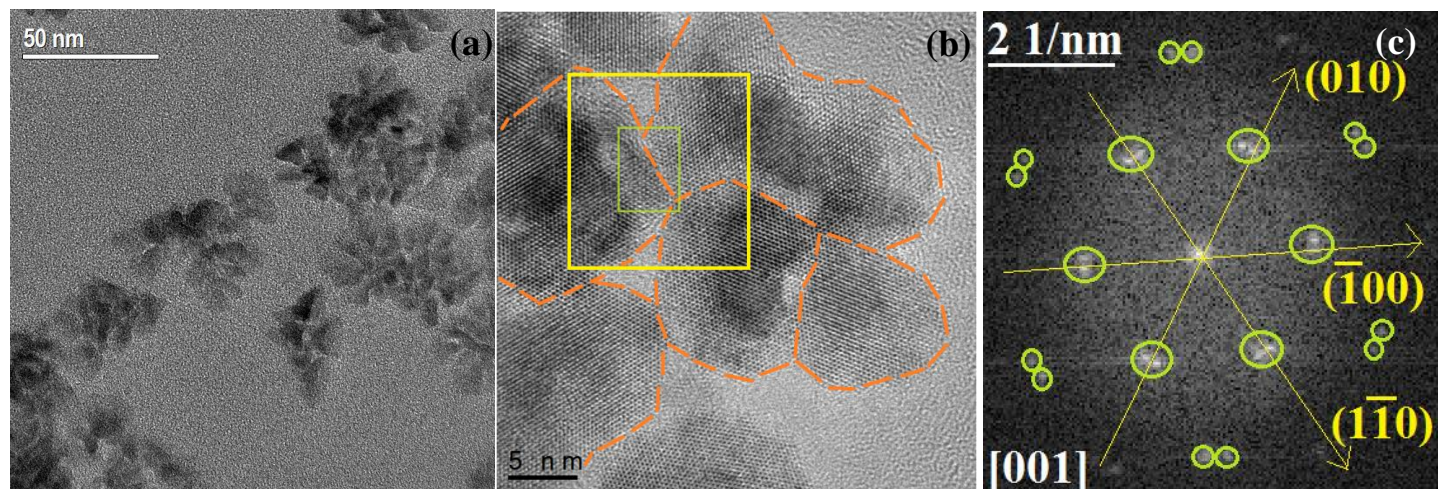


Fig. S3: Atomic model of crystal planes of two different nanocrystals along (010) axis showing the attachment of Zn<sup>2+</sup> rich {002} facet of one with O<sup>2-</sup> rich {002} facet of another NC. Cyan: Zn, Red: oxygen.



**Fig. S4:** Atomic model of ZnO showing incorporation of  $Mg^{2+}$  ions in the interstitial position and the {110}, {010} and {1-10} facets.



**Fig. S5:** (a) TEM image of 20% Mg alloyed ZnO sample quenching the reaction after 15 sec. (b) Each grain size was found to be in 5-10 nm size region. The grain boundary has been highlighted. (c) FFT pattern from yellow squared area shows the presence of twin planes: initiation of oriented attachment.

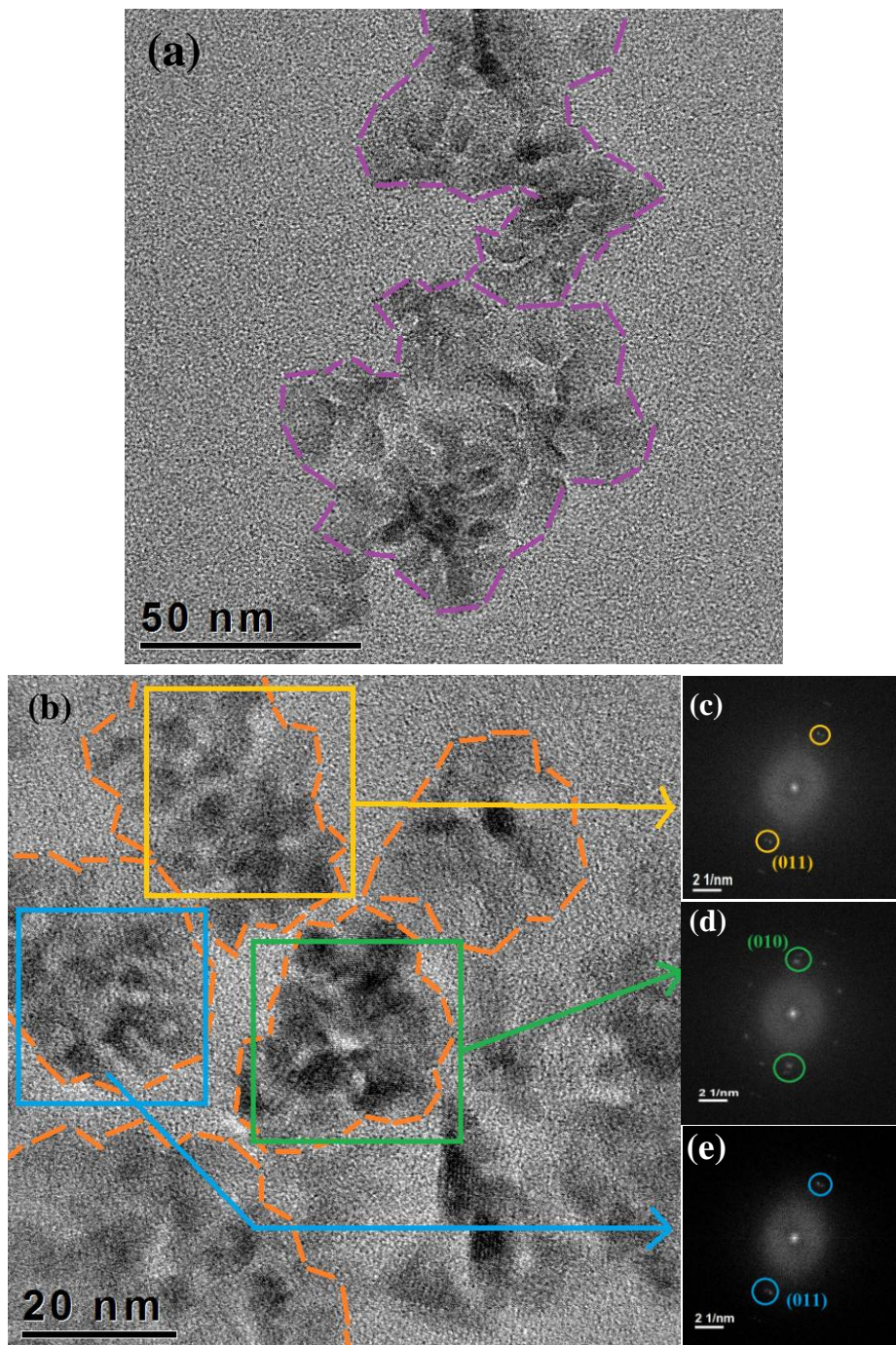


**Fig. S6:** (a) TEM image of 20% Mg alloyed ZnO sample after 1 min of reaction. (b) Closer View of a cluster which was formed by self assembly of small nano-assemble (in Fig. S5). The grain boundary has been highlighted. (c-e) FFT patterns of different grain boundary areas.

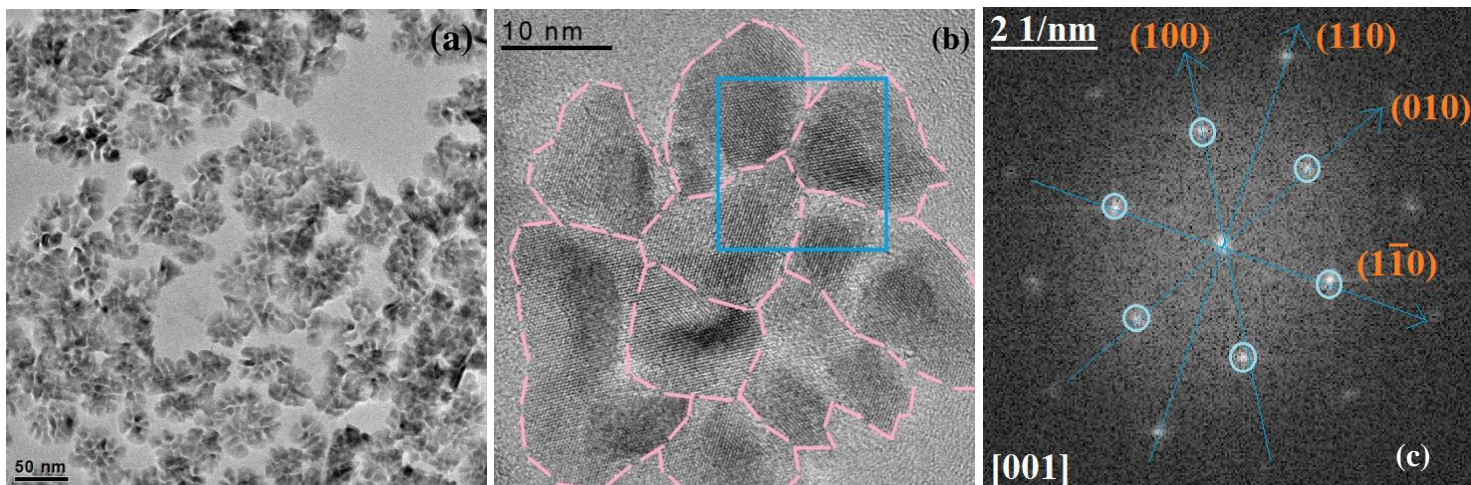
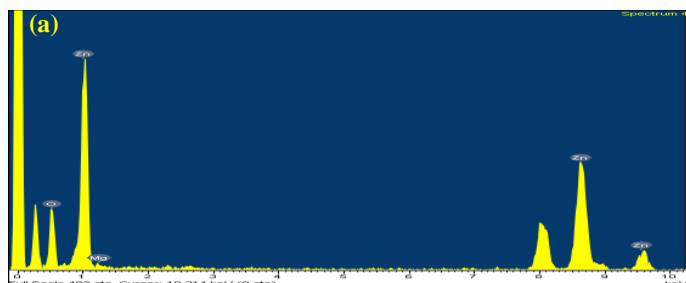
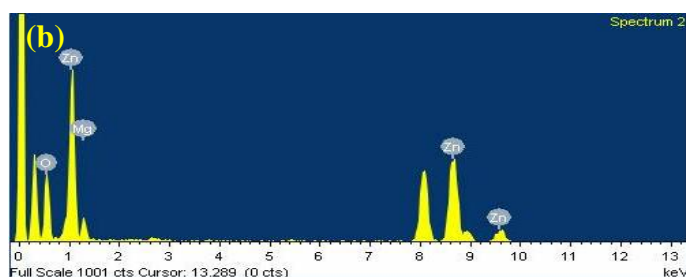


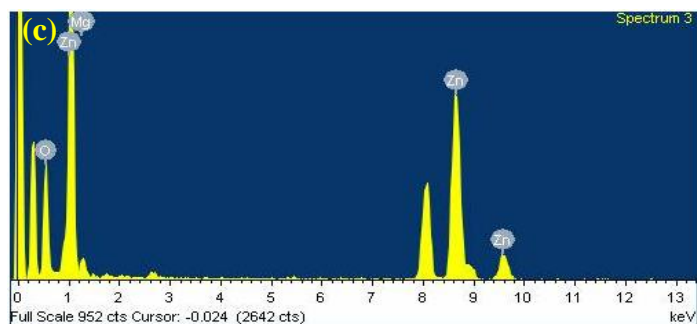
**Fig. S7:** (a) TEM image of 20% Mg alloyed ZnO sample after 10 min of reaction. (B) A closer view of a single cluster shows the assembly of 8 - 9 small NCs. (c) FFT of blue squared area shows nearly single crystalline nature.



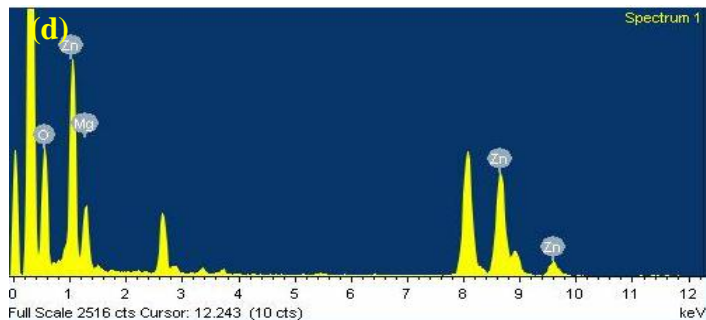
Element	Peak Area	Area Sigma	k Factor	Abs Corr.	Weight %	Weight %Sigma	Atomic %
O K	747	51	1.810	1.000	20.03	1.34	54.57
Mg K	45	20	1.085	1.000	0.83	0.37	1.29
Zn K	3118	96	1.434	1.000	76.14	1.36	44.14
Totals					100		



Element	Peak Area	Area Sigma	k Factor	Abs Corr.	Weight %	Weight %Sigma	Atomic %
O K	1866	79	1.810	1.000	26.81	0.93	58.50
Mg K	311	44	1.085	1.000	2.68	0.37	3.84
Zn K	6196	133	1.434	1.000	7.52	0.96	37.66
Totals					100		



Element	Peak Area	Area Sigma	k Factor	Abs Corr.	Weight %	Weight %Sigma	Atomic %
O K	1298	65	1.810	1.000	29.63	1.20	59.76
Mg K	483	45	1.085	1.000	6.61	0.59	8.77
Zn K	3525	102	1.434	1.000	63.76	1.23	31.47
Totals					100		



Element	Peak Area	Area Sigma	k Factor	Abs Corr.	Weight %	Weight %Sigma	Atomic %
O K	5958	151	1.810	1.000	40.75	0.75	67.43
Mg K	3059	119	1.085	1.000	12.54	0.46	13.66
Zn K	8622	175	1.434	1.000	46.70	0.74	18.91
Totals					100		

**Fig. S8:** (a)-(d) EDAX analysis shows the Mg% increases in  $Zn_{1-x}Mg_xO$  samples (5%, 10%, 20%, 30% respectively).

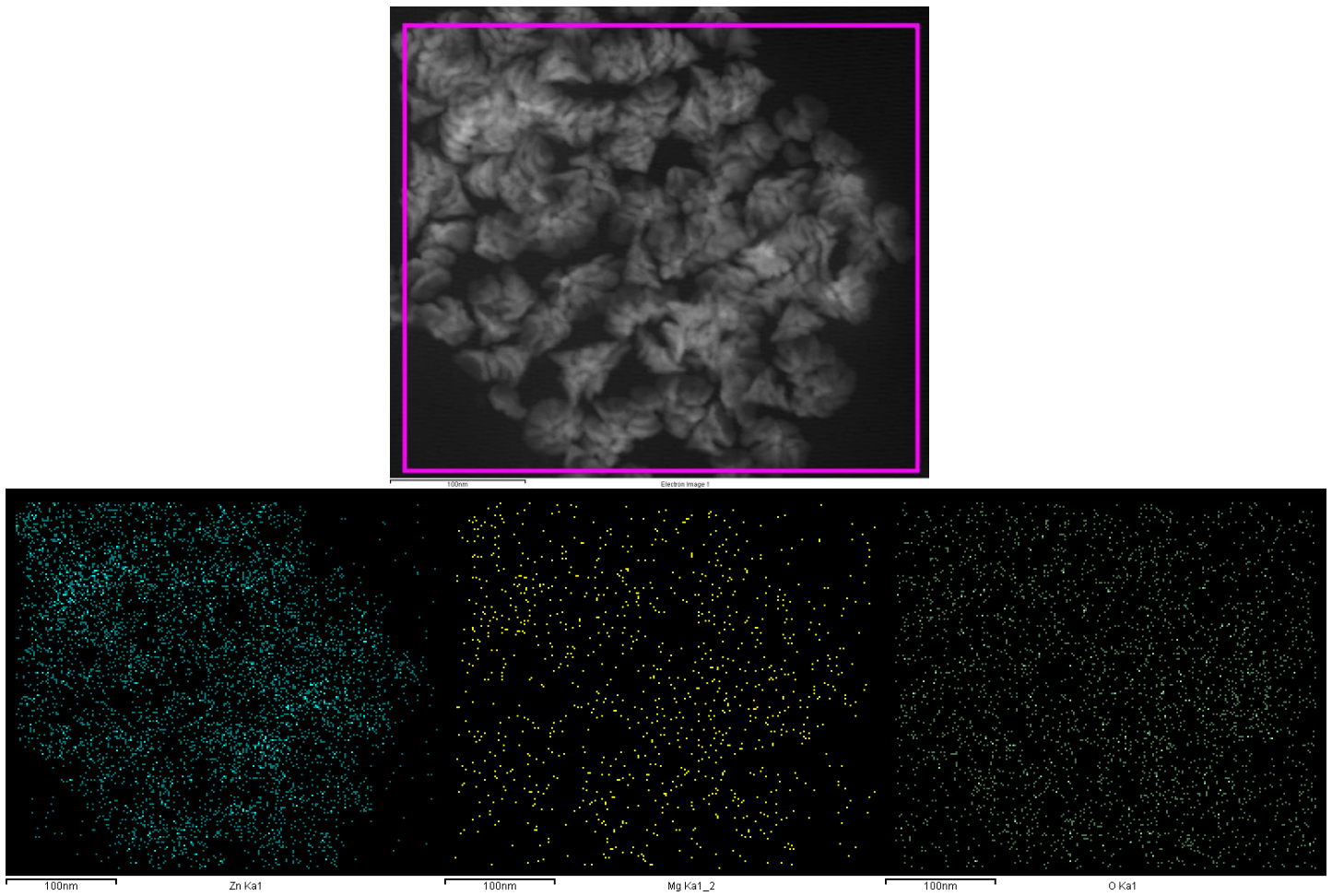


**Fig. S9:** EDS-element mapping of 20% Mg alloyed ZnO nano-assembly.



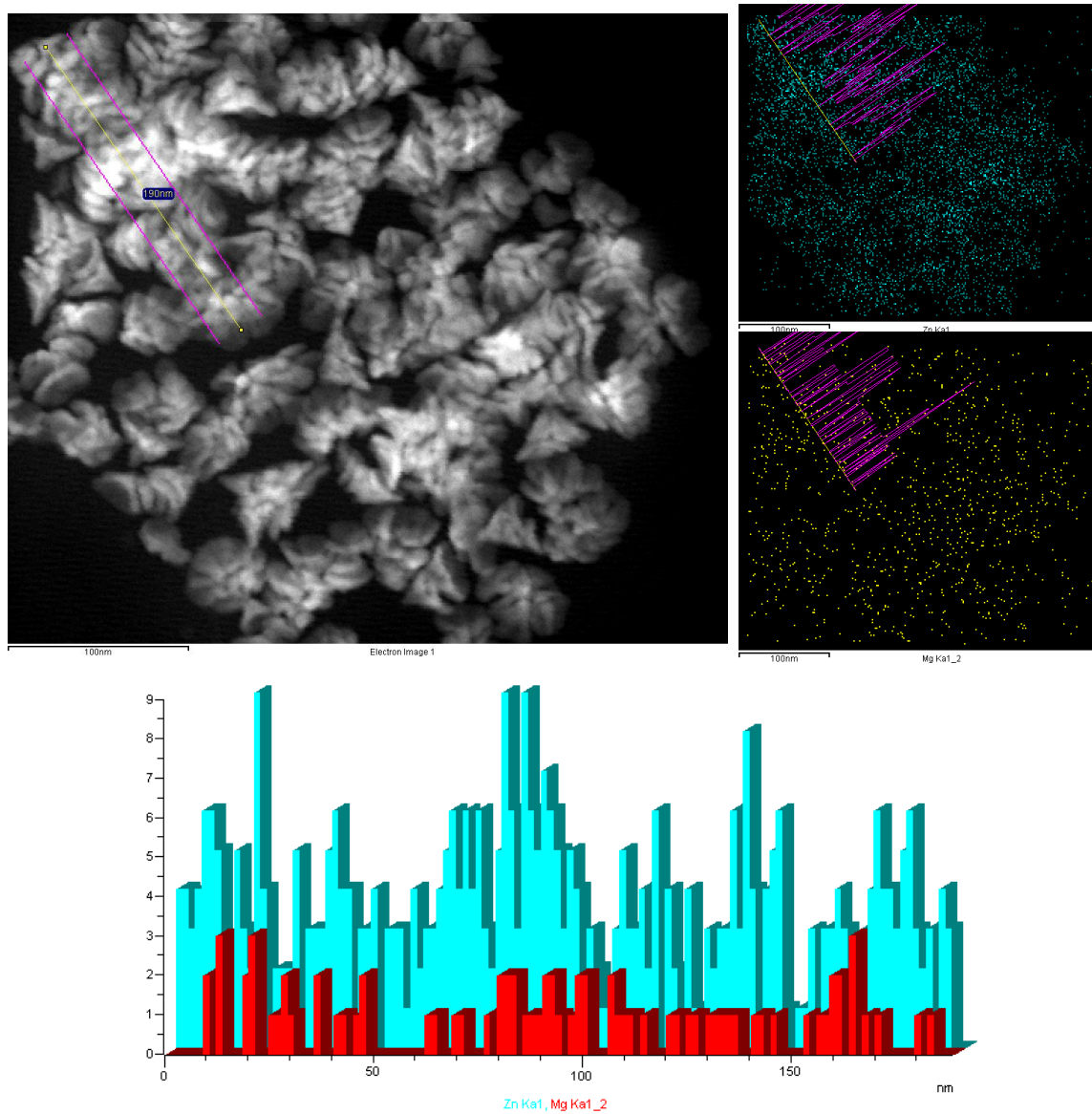


**Fig. S10:** Line scan over 4-5 number of 20% Mg alloyed ZnO assembly. Periodic presence of high Mg% where the Zn% is low.

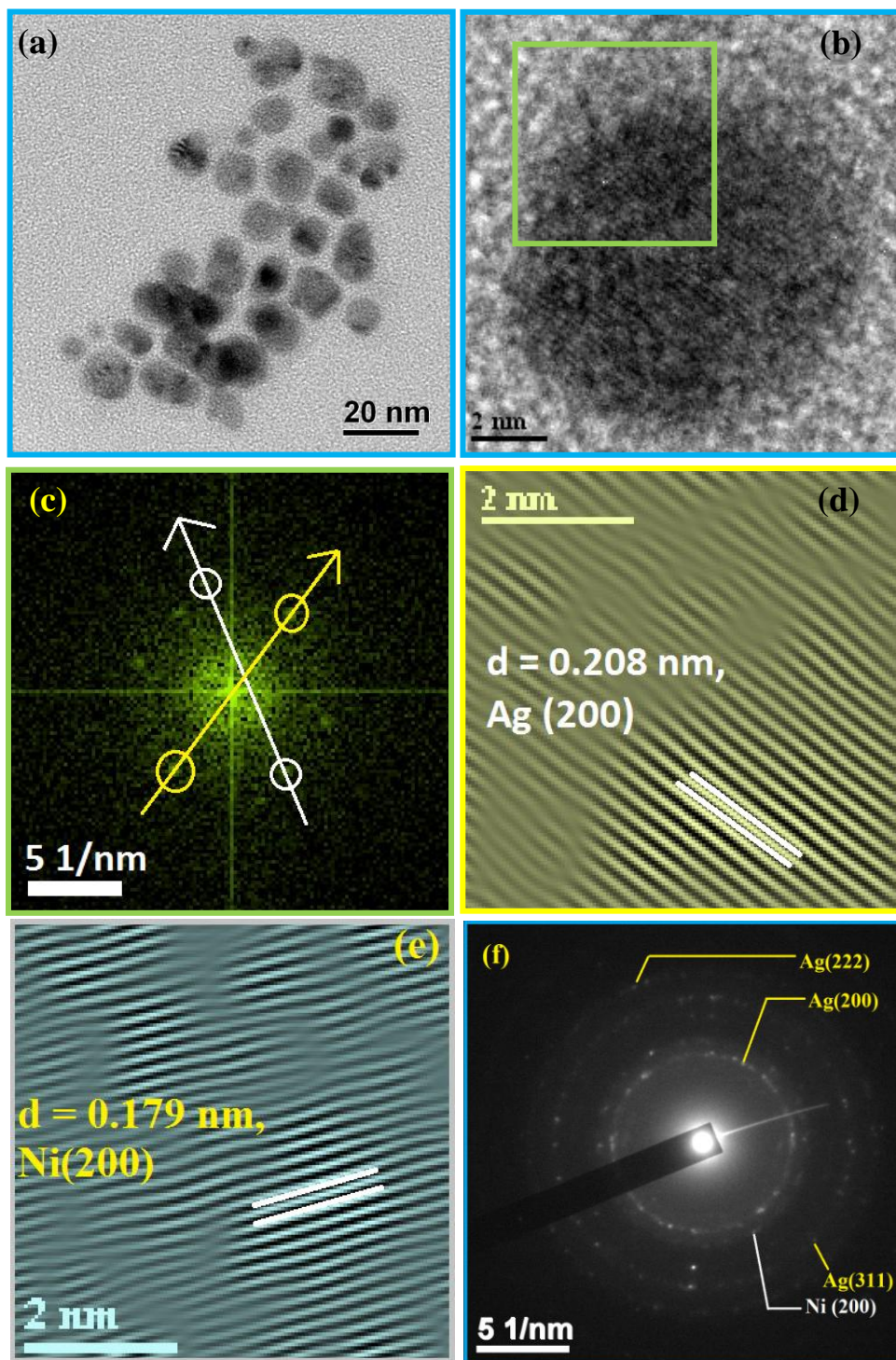


**Fig. S11** : (a) Large area TEM image of Ag@Ni core shell nanostructures. (b) HRTEM image of a single core shell structure. (c) FFT pattern of the interface area (green marked area in Fig. b). (d) reconstructed HRTEM image of Ag. (e) reconstructed HRTEM of Ni showing (200) planes. (f) SAED pattern of Ag@Ni nanocrystals.

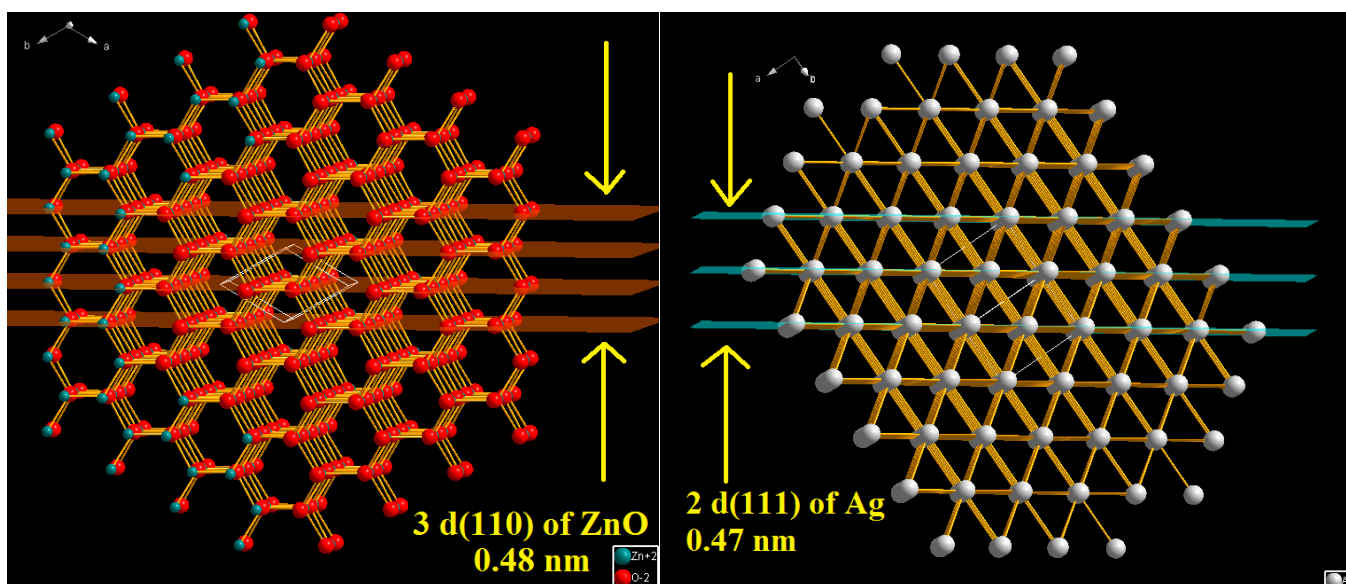


**Fig. S12:** shows the atomic model of the matching of  $3 \times d(110)$  of ZnO with  $2 \times d(111)$  of Ag plane.

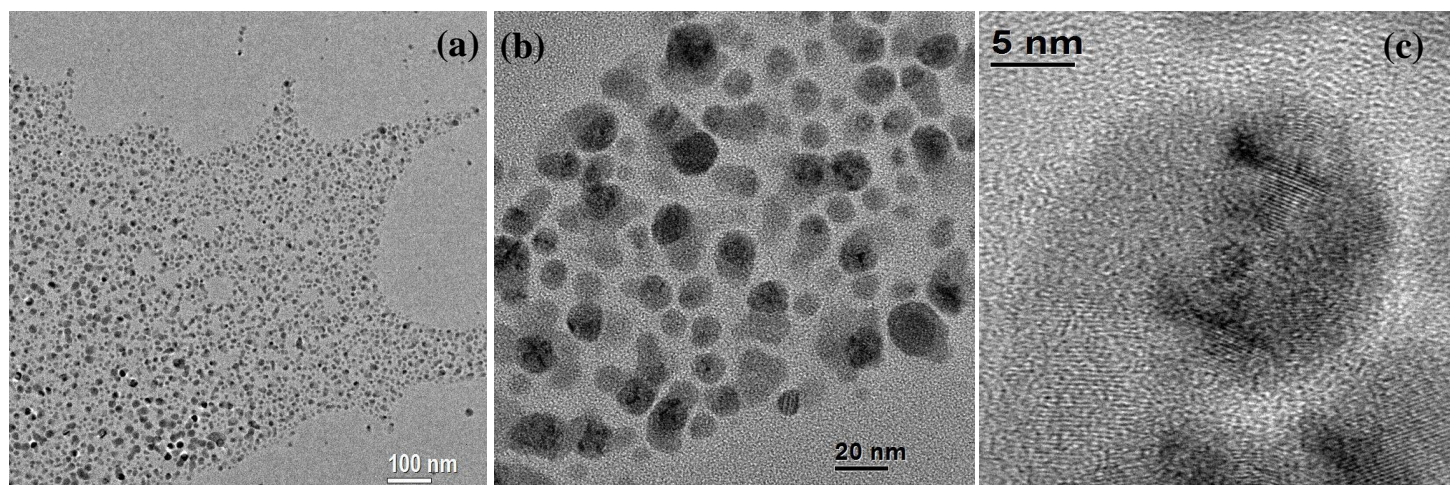


**Fig. S13:** (a) TEM image of Ag@Ni/Zn<sub>0.8</sub>Mg<sub>0.2</sub>O sample collected at 10 min of reaction. (b) Closer View shows all the metal nanocrystals are situated with ZnO part (lower contrast) with some free standing ZnO nanocrystals. (c) HRTEM image of Ag-ZnO heterodimer.

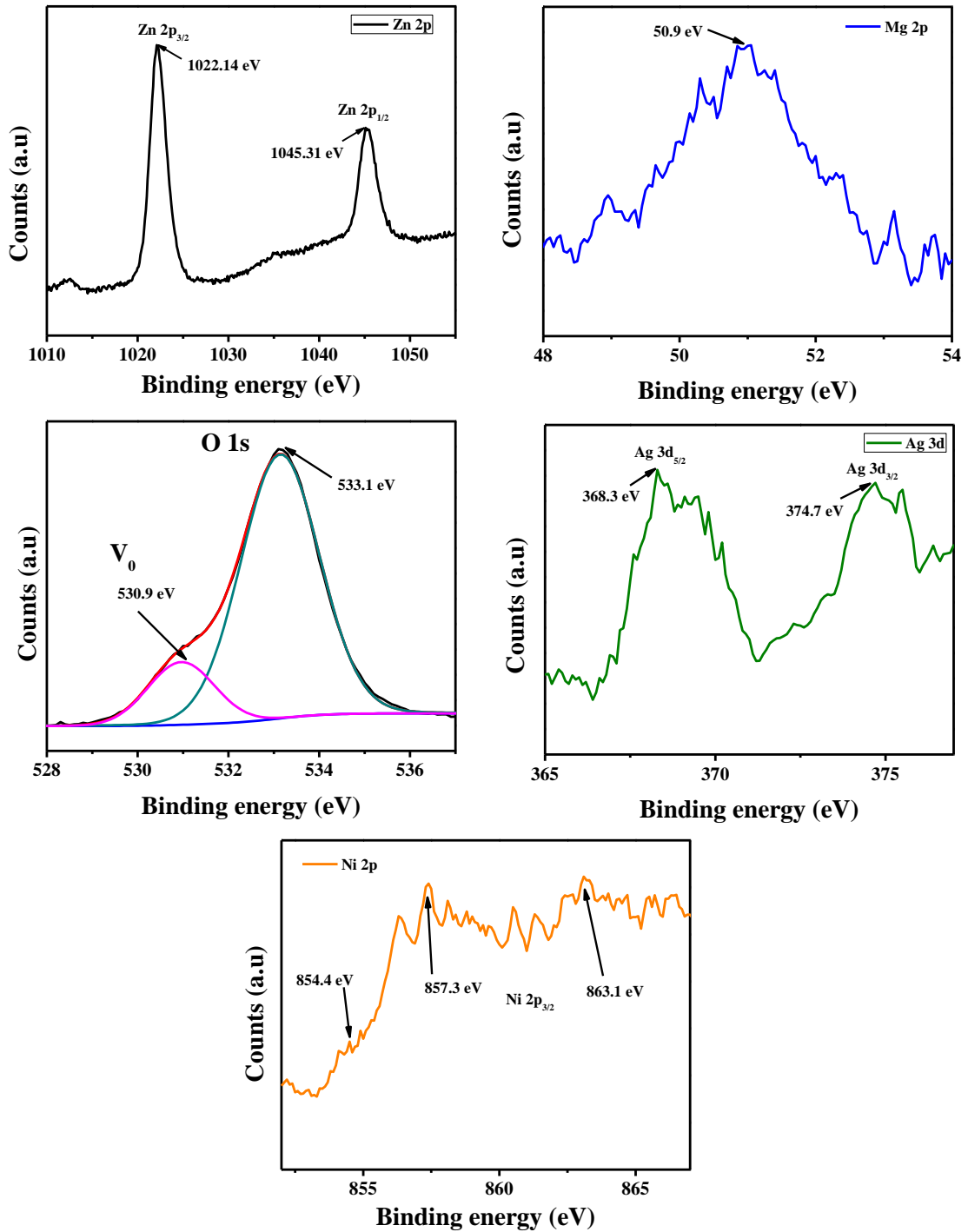


**Fig. S14:** XPS spectra of Ag@Ni/Zn<sub>0.8</sub>Mg<sub>0.2</sub>O heterostructure.

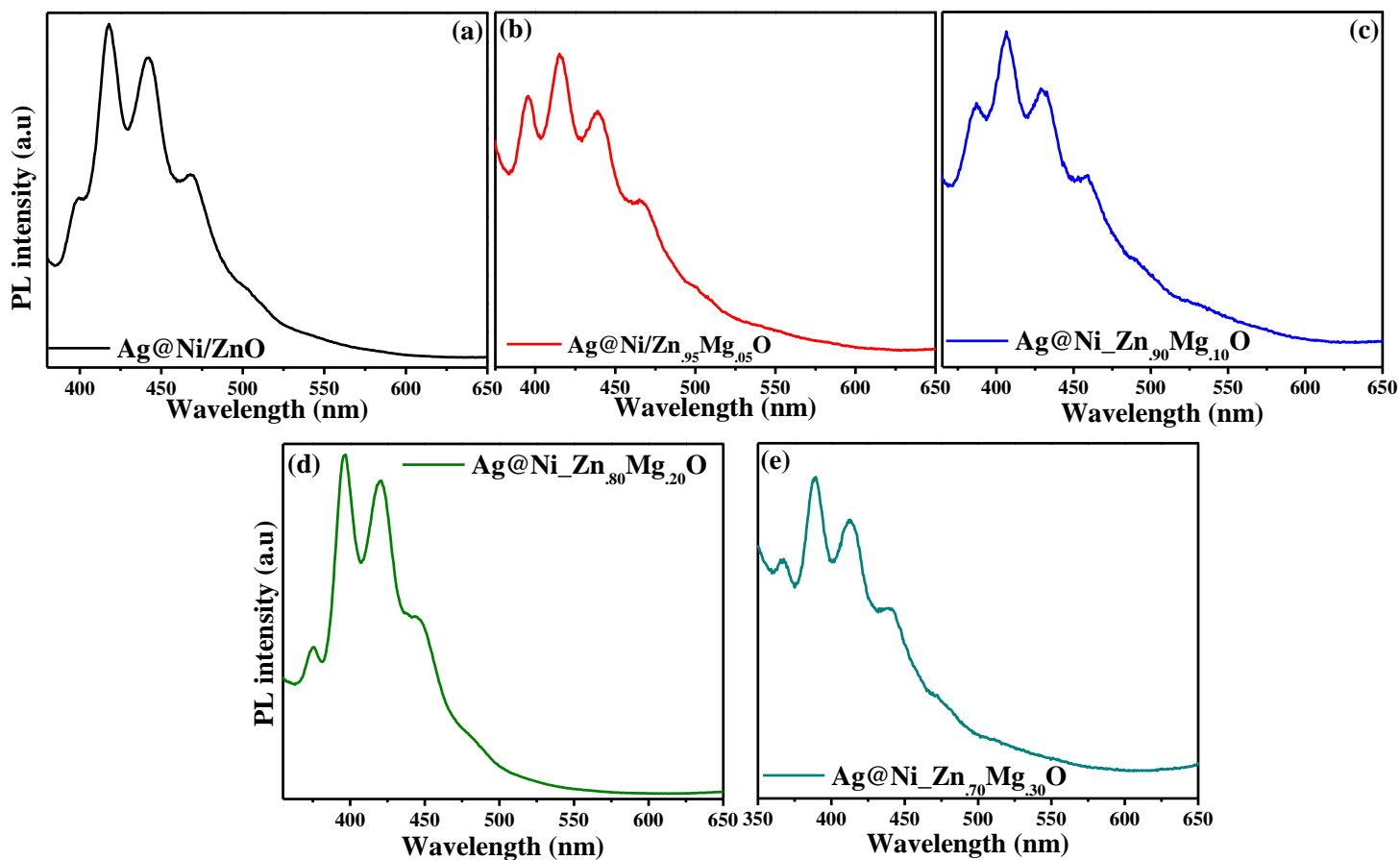


**Fig. S15:** PL spectra of Ag@Ni decorated ZnO and  $Zn_{1-x}Mg_xO$  samples.

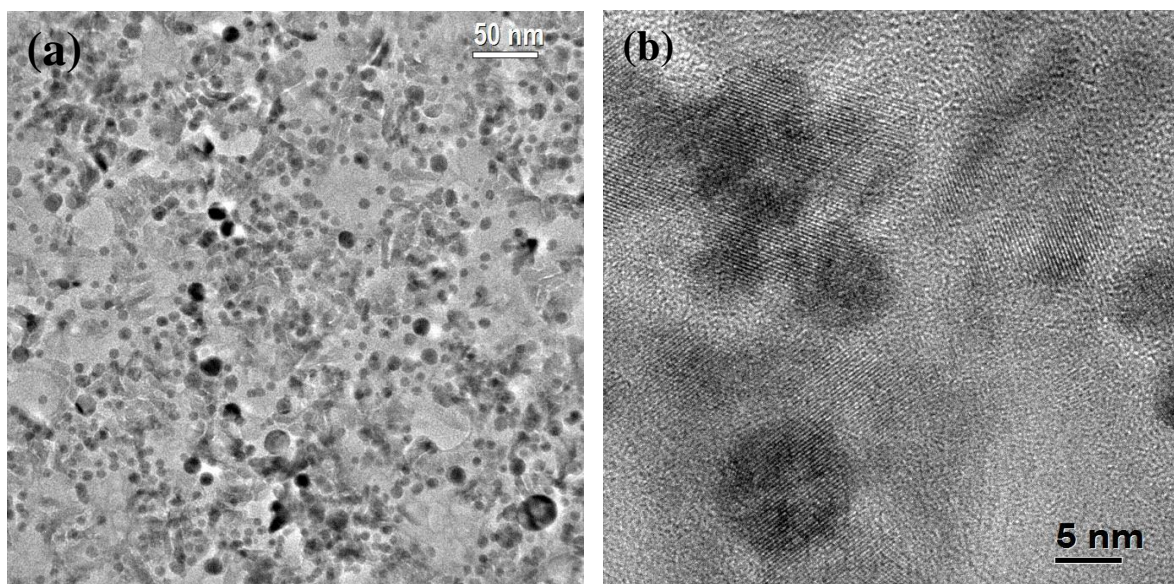


**Fig. S16:** (a) Large area and Closer view of Ag@Ni/ $Zn_{0.7}Mg_{0.3}O$  heterostructure shows the morphology of sample is sheet like and decorated with multiple number of metal particle.



**Fig. S17:** Separation of Ag@Ni/Zn<sub>0.8</sub>Mg<sub>0.2</sub>O NHS catalyst by magnetic bar.

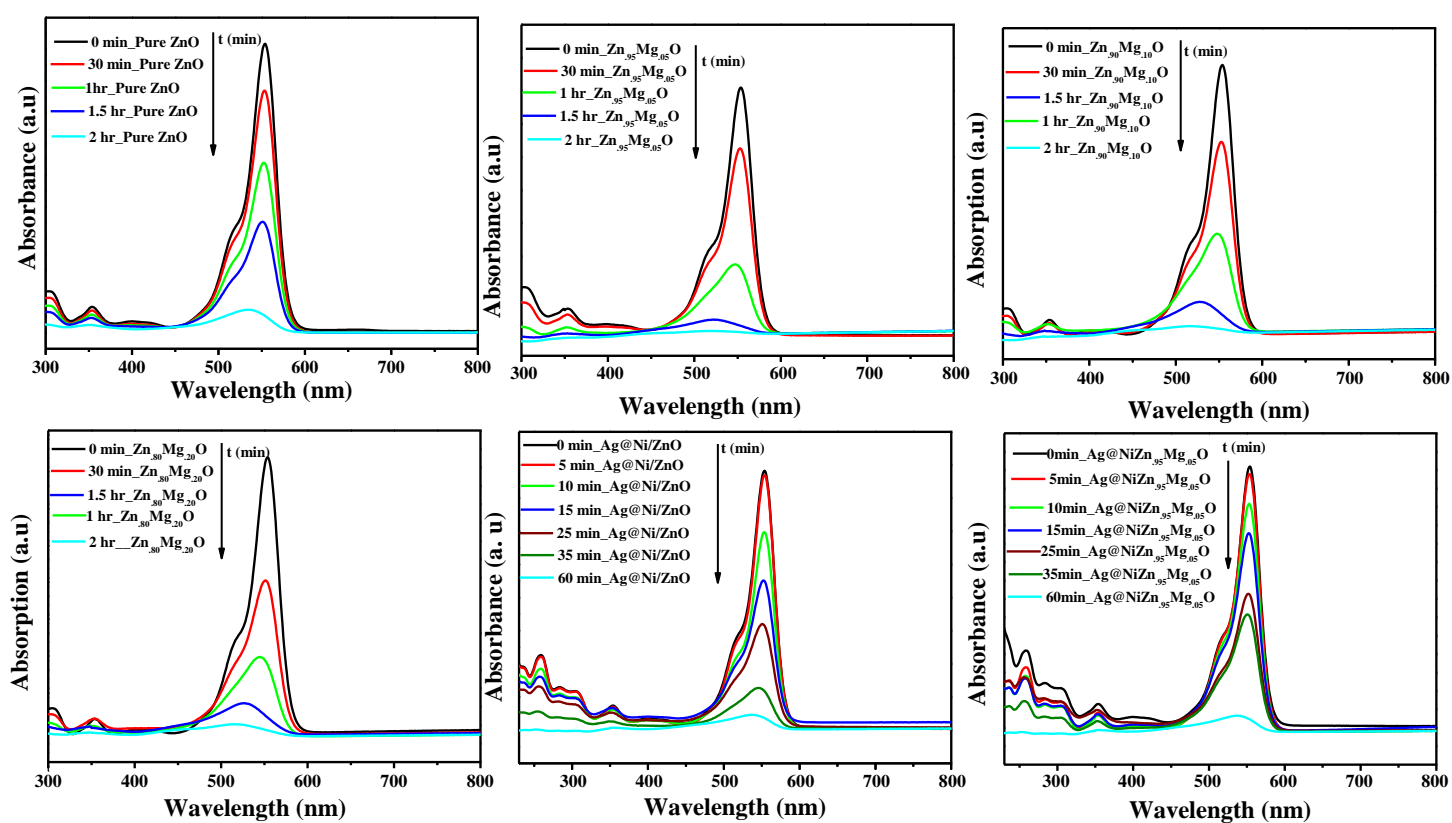


**Fig. S18:** Degradation of RhB dye in presence of different catalyst.

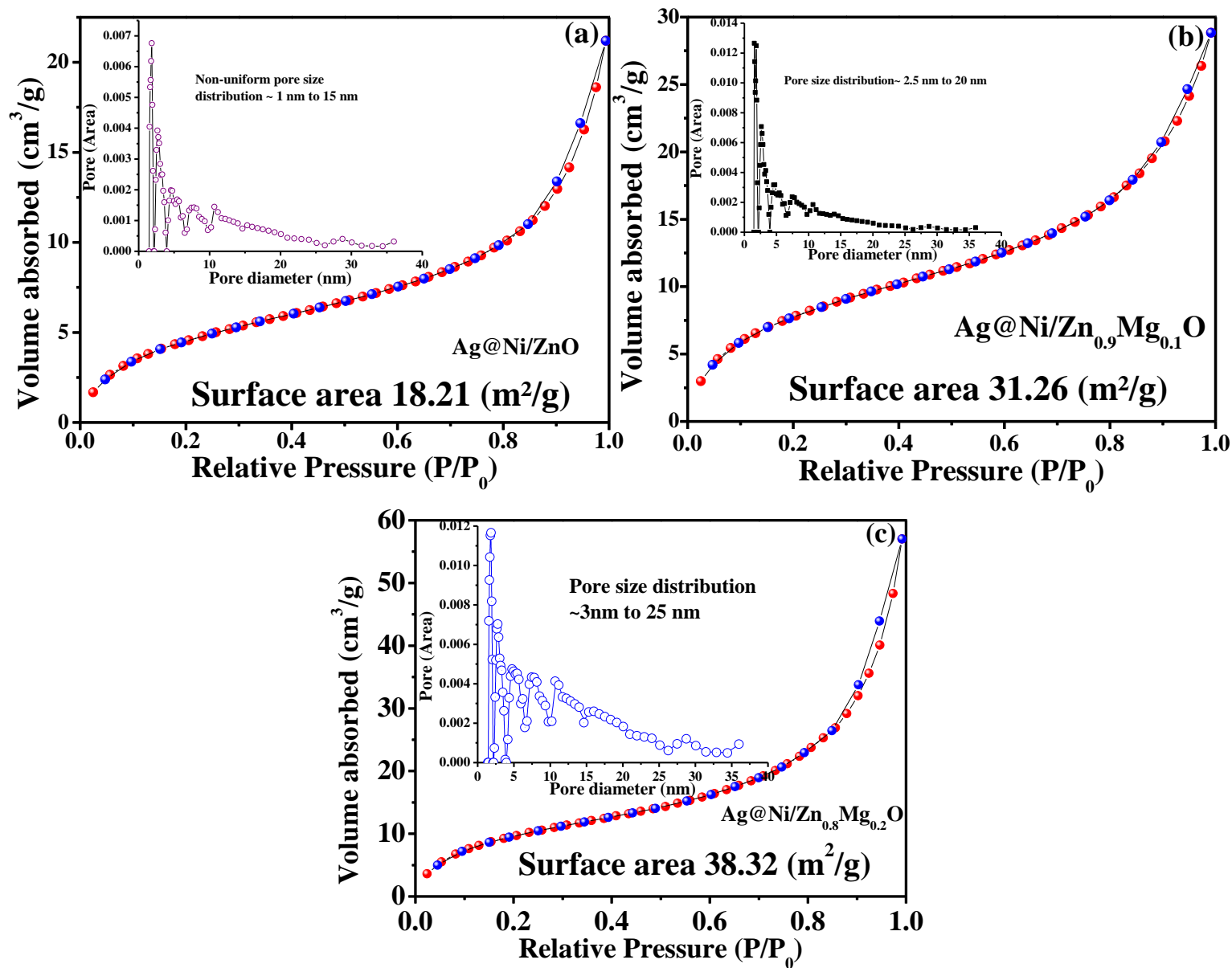


**Fig. S19:** BET adsorption–desorption isotherms and the pore-size distribution (inset) of (a) Ag@Ni/ZnO, (b) Ag@Ni/Zn<sub>0.9</sub>Mg<sub>0.1</sub>O and (c) Ag@Ni/Zn<sub>0.8</sub>Mg<sub>0.2</sub>O heterostructures.

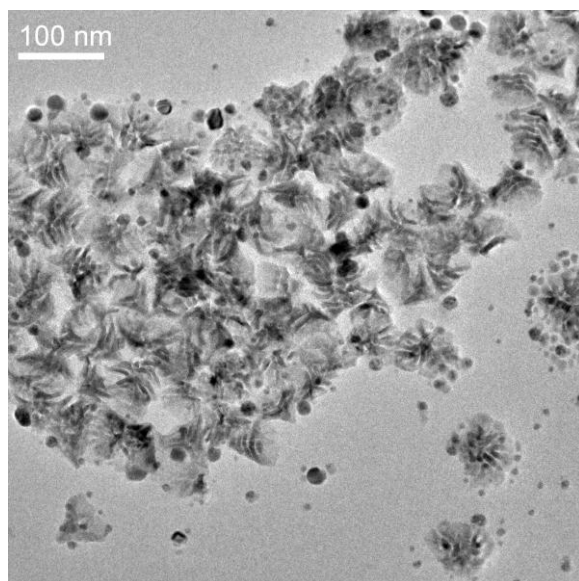


**Fig. S20:** Tem image of the recovered Photocatalyst Ag@Ni/Zn<sub>0.8</sub>Mg<sub>0.2</sub>O NHSs



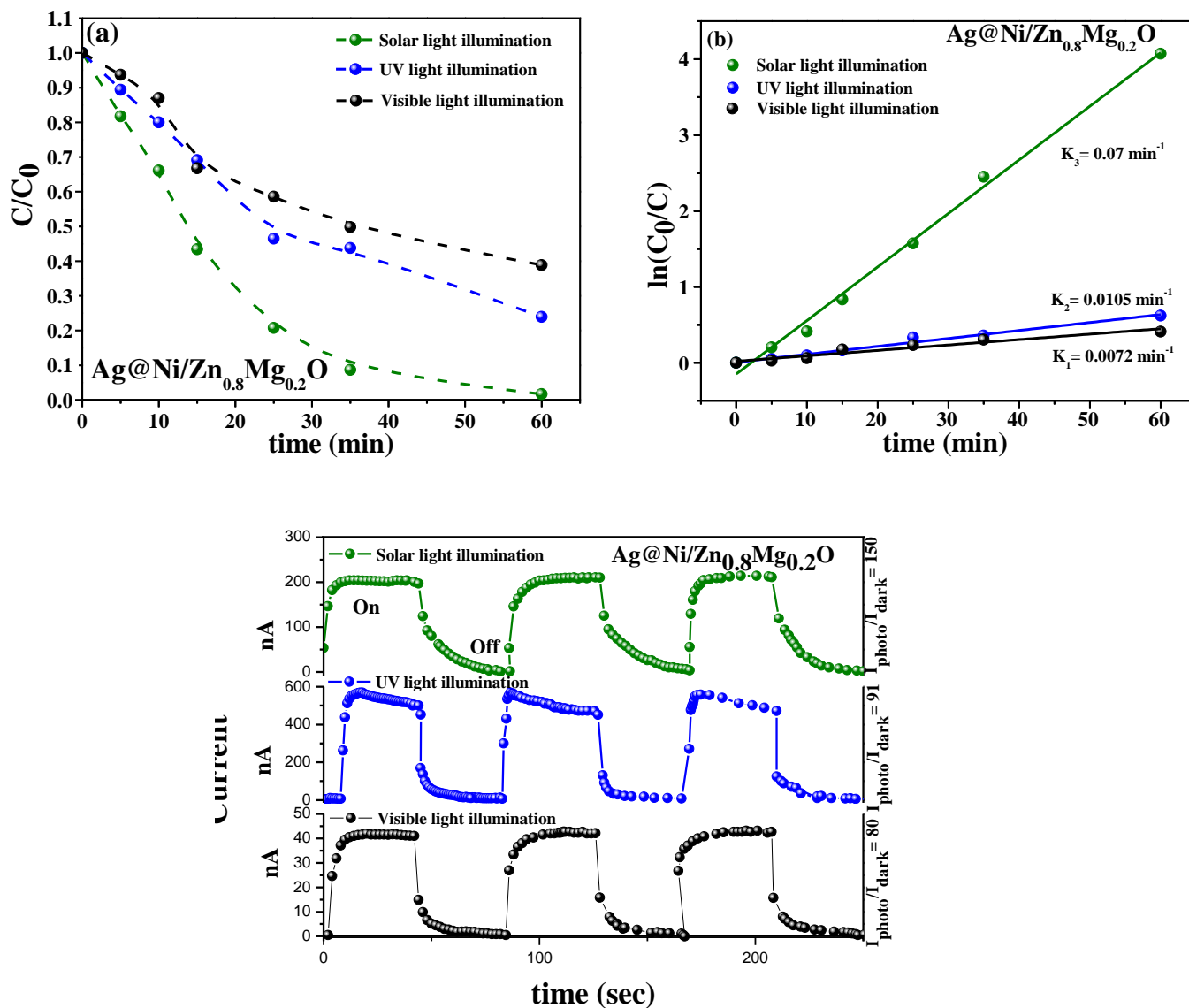


**Fig. S21:** (a) Photocatalytic activity of  $\text{Ag@Ni/Zn}_{0.8}\text{Mg}_{0.2}\text{O}$  under different light excitation, (b) rate constant of same and (c) photo response of same.